January 2008 Volume 4 Issue 2

Trade Science Inc.

Materials Science

An Indian Journal

Full Paper

MSAIJ, 4(2), 2008 [95-99]

Ferroelectric and dielectric property of $BiFeO_3$ films on different bottom electrodes

Liu Hongri*, Wang Xiuzhang

Department of Physics, Hubei Normal University, Huangshi-435002, (P.RCHINA)

E-mail: lhr1229@126.com

PACS: 77.55.+f, 77.80-e

Received: 9th January, 2007 ; Accepted: 14th January, 2007

ABSTRACT

$BiFeO_3$ films have been prepared on $LaNiO_3$, indium tin oxide (ITO) and Pt bottom electrodes by the sol-gel process. The films on different bottom electrodes were prepared at an annealing temperature of 550^0C. X-ray diffraction patterns indicate that all films adopt R3m structure and different orientation on different substrates. No impure phases were identified in the films in different bottom electrodes. Cross section scanning result shows that the thickness of the films is about 350nm. Room temperature ferroelectricity was observed by measuring electric hysteresis loops. The film on $LaNiO_3$ bottom electrodes has the largest double remnant polarization 6.61 $\mu C/cm^2$. The remnant polarizations are 4.14$\mu C/cm^2$ and 4.53$\mu C/cm^2$ for the films on ITO and Pt bottom electrodes respectively. More over, the films on Pt and ITO bottom electrodes show small dielectric dispersion and the film on ITO bottom electrode has least leakage conduction at the same applied field.

KEYWORDS

Sol-gel;
Ferroelectricity;
$BiFeO_3$ film;
Dielectric property;
Leakage current.

INTRODUCTION

In recent years, a new class of materials has attracted extensive attentions, in which both electrical and magnetic ordering can coexist. They are called multiferroic materials and exhibit coexistence of magnetic and ferroelectric ordering in a certain temperature range. Multiferroic materials are important for realizing multifunctional devices used in information storage, spintronics, and so on[1-3]. As a typical multiferroic material, $BiFeO_3$ is reported to exhibit about eight structure transitions[4] and a weak antiferromagnetic ordering (T_N=397^0C) and ferroelectric ordering (T_C=850^0C) [5]. Its semiconducting nature at room temperature does not allow proper electrical poling leading to high dielectric loss[6]. In addition, during synthesis, the kinetics of formation always leads to a mixture of $BiFeO_3$ as a major phase along with other impurity phases[7]. The lattice structure of a $BiFeO_3$ bulk single crystal is a rhombohedrally distorted perovskite, which belongs to the space group R3c with unit-cell parameters a=0.396nm and =89.4^0C[8].

Recently, enhanced ferroelectric properties have been reported in $BiFeO_3$ thin films fabricated by pulsed laser deposition[9,10] and chemical solution deposition[11] although it is difficult to measure electrical properties at room temperature because of their low resistance. The large remnant polarization in $BiFeO_3$ thin films was initially thought to be a stress-induced property[9], but more recently it is interpreted to be an intrinsic property which even appears in unstressed films[12]. In fact, in view of preparation technology, there are some factors are responsible for the ferroelectricity of $BiFeO_3$ films such as deposition atmosphere in pulsed laser deposition method and magnetron sputtering method, precursor solution in sol-gel process and etc. Despite the preparation method, bottom electrode is a very important factor to the electric and magnetic property of $BiFeO_3$ film since different bottom electrodes may produce different interface layers which determine the leakage conduction of the film/substrate system. Furthermore, perovskite $BiFeO_3$ can epitaxial growth on prevoskite bottom electrode and obtained enhanced ferroelectricity for stress[1]. While to our knowledge, there is seldom work has been focused on the properties of $BiFeO_3$ films on different bottom electrodes.

In the present work, we prepared $BiFeO_3$ films on conductive oxygen bottom electrode and Pt bottom electrode. The effects of different bottom electrodes on the orientation, microstructure, ferroelectric property and dielectric property are studied.

EXPERIMENTAL

The $BiFeO_3$ films were prepared on $LaNiO_3/SiO_2/Si$, indium tin oxide (ITO)/glass and $Pt/Ti/SiO_2/Si$ substrates by sol-gel process. The preparation method of $LaNiO_3/SiO_2/Si(111)$ is given in[13]. The ITO/glass and $Pt/Ti/SiO_2/Si$ substrates are commercial purchased. Before spin coating the three substrates were cleaned by ultrasonication in alcohol and acetone repeatedly. The $BiFeO_3$ precursor solutions were prepared using bismuth nitrate[$Bi(NO_3)_3{\cdot}5H_2O$] and iron nitrate [$Fe(NO_3)_3{\cdot}9H_2O$] as staring materials. Bismuth nitrate and iron nitrate were mixed with a molar ratio of 1:1 and dissolved at room temperature in 2-methoxyethanol and stirred for 30 minutes. Then sufficient acetic anhydride was added to dehydrate and ethanolamine was added to adjust the viscosity under constant stirring. The concentration of the stock solutions was adjusted to 0.3M by adding 2-methoxyethanol. The above processes were performed in an ambient atmosphere at room temperature. The depositions were carried out by spin coating at 6000 rpm for 15s. The as deposited wet films were pre-annealed at 350^0C for 3 minutes and followed by an annealing at 550^0C in air for 3 minutes. The above procedures were repeated several times to obtain the desired thickness.

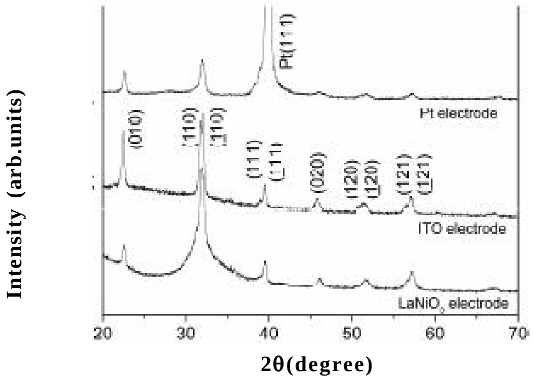

Figure 1 : XRD patterns of the films on different bottom electrodes

The structure of the films was analyzed by XRD. The XRD patterns were recorded with X-ray diffractometer with CuKα radiation. The morphology was analyzed by scanning electron microscopy. For electrical measurements, Pt dots of $0.1mm^2$ were deposited through a mask on the films by sputtering. Before measuring, the films were annealed at 300^0C for 20 minutes to get full contact with the electrodes. Dielectric property was measured with a HP 4284A LCR meter. Ferroelectricity loops and leakage currents were obtained using a precision work station (Radiant Technology).

RESULT AND DISCUSSION

The crystalline nature of the films was identified by XRD. Figure 1 shows the XRD patterns of the $BiFeO_3$ films on different substrates annealed at 550^0C; the pattern of the $BiFeO_3$ films is identified according to ICCD 20-0169. The films are fully crystallized since high intense peaks are evident and no impure phase such as $Bi_2Fe_4O_9$ are spotted in the films on different substrates. In addition, rhombohedral perovskite structure was identified since the XRD patterns match to the standard pattern quite well. Although we did not obtain highly preferred oriented films on different bottom, the variation of (110) and (110) peak is obvious. In $BiFeO_3$,

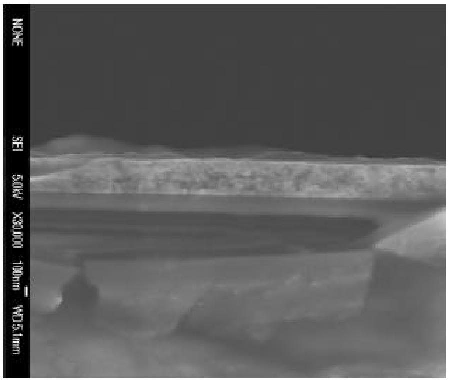

Figure 2 : Croos section scanning electric microscopy phots of the film on ITO bottom electrode.

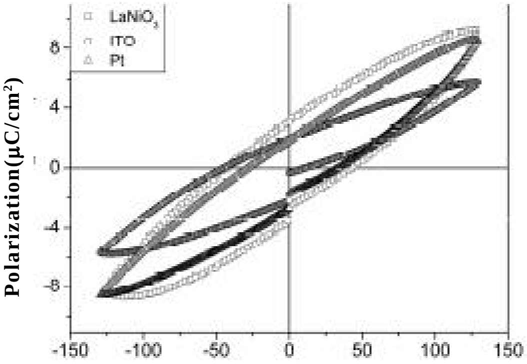

Figure 3 : Electric hycteresis loops of $BiFeO_3$ films on different bottom electrides

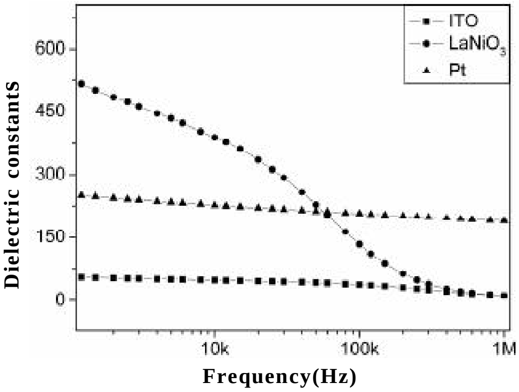

Figure 4 : Dielectric constant Vs. frequency relation

the(110) and (110) peaks are originated from the split of(110) peak of cubic perovskite structure because of the stretch of $BiFeO_3$ unit cell along(110) direction. The film on $LaNiO_3$ bottom electrode has the most intense (110) and (110) peaks and it is called (110)and (110) biaxis preferential orientation[14], while the films on ITO and Pt bottom electrodes are randomly orientated. Our results are different from that of Iakovlev's. In their work, (100) preferred oriented film were prepared on Pt bottom electrodes by chemical solution deposition method. The orientation of the film is determined by some factors such as crystal lattice match, stress, surface effects and etc. According to our previous work, there is possibility of crystal lattice match between the $BiFeO_3$ film and $LaNiO_3$ bottom electrode[14]. In our work, the $LaNiO_3$ bottom electrode are (100) preferred oriented (the XRD is shown elsewhere) while the $BiFeO_3$ film are (110) and (110) biaxis preferential orientation, it means that the orientation is not determined by crystal lattice match in the $BiFeO_3$/$LaNiO_3$ system. Stress is very likely responsible for it. As for the film on ITO bottom electrode, there is no crystal lattice match between the noncrystal ITO bottom electrode and perovskite $BiFeO_3$ bottom therefore we can expect the random orientation. We think that the random orientation of $BiFeO_3$ film on Pt bottom electrode is mainly determined by the preparation technology.

In order to confirm the thickness, a cross section SEM for the film on ITO bottom electrode was done. Figure 2 shows the cross section SEM photo of the $BiFeO_3$ film. Through which the film is confirmed to have a homogenous thickness and the thickness, according to figure 2, is about 350nm. Moreover, a compact intermediate layer of about 100nm can be easily identified in the film.

The ferroelectric hysteresis loops are shown in figure 3. All films show well hysteresis character. For comparison, the electric hysteresis loops are measured at a same applied field of 128kV/cm. It is obvious that the film on different bottom have different remnant polarization. The double polarization(2Pr) values are 6.61μC/cm², 4.53μC/cm² and 4.14μC/cm² for the films on $LaNiO_3$, Pt and ITO bottom electrodes respectively. It is well known that the ferroelectricity in $BiFeO_3$ films are originated from the relative displacements of Bi ion and Fe-O octahedron[1] and the projection polarization along the (110) orientation is larger than that of the (100) orientation[9]. According to figure 1, the (110) and (110) peaks of the films on different bottom electrodes have different relative intensity in the XRD patterns. The film on $LaNiO_3$ bottom electrode has the largest relative intensity therefore has the largest 2Pr; the film on Pt bottom electrode has the larger relative intensity and it

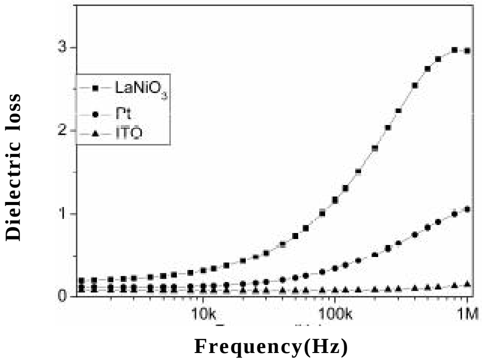

Figure 5 : Dielectric constant Vs. frequency

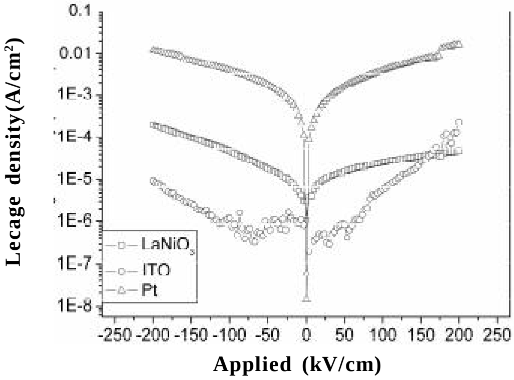

Figure 6 : J-E characteristics of BiFeO$_3$ films on varied bottom electrodes

ally therefore the dielectric constant decreases with the frequency. At high frequency, according to Chopra[16], the falling in dielectric constant arises from the fact that polarization does not occur instantaneously with the application of the electric field because of inertia. As frequency is increased, those with large relaxation times cease to respond and hence the decrease in dielectric constant. It also can be seen that the three films have different dielectric constant at same measuring frequency. It is well known that the dielectric constant is determined by the polarization in ferroelectrics. Since the films on LaNiO$_3$ and Pt bottom electrode has more intense polarization than the one on ITO bottom, we expect larger dielectric constant for them.

The dielectric loss-frequency relation is shown in Figure 5, all films have low dielectric loss at low frequencies and the dielectric loss increase drastically above 10 kHz for the films on LaNiO$_3$ and Pt bottom electrode. The film on ITO bottom electrode has small dielectric loss at the whole frequency range. The dielectric loss show a small decrease at low frequency for the films on ITO and Pt bottom electrodes and it is suggested to originate from the DC conduction. The film on LaNiO$_3$ bottom electrode has the largest dielectric loss at the whole frequency range. A dispersion peak was observed near 1MHz and it may be from a new dispersion mechanism caused by the intermediate layer.

We also studied the leakage current characteristic of the BiFeO$_3$ films on different electrodes. Positive and negative bias voltages were applied to the top electrodes and the J-E curves were recorded. Figure 6 shows that the leakage current density for the film on Pt bottom electrode is about two magnitude orders lager than that of the film on LaNiO$_3$ bottom electrode. In BiFeO$_3$, larger leakage current density is well known caused by oxygen vacancies originated from the valence decrease of Fe^{3+} to Fe^{2+}[17]. The J-E curve has well symmetry for the film on Pt electrode and it is attributed to the symmetrical Pt bottom electrode and top electrode. The result is similar to that of BiFeO$_3$ films deposited by pulsed laser deposited at different oxygen pressures on Pt bottom electrode[18]. The J-E curves are asymmetrical for the film on LaNiO$_3$ and ITO bottom electrode and it is attributed to the asymmetry of bottom electrode and Pt top electrode. The BiFeO$_3$ film on ITO bottom electrode has the least leakage current density and it is attributed to the compact intermediate layer (see figure 2).

CONCLUSIONS

BiFeO$_3$ films were deposited on LaNiO$_3$, Pt and ITO bottom electrodes by sol-gel process. Biaxial preferred and randomly oriented films were obtained at an annealing temperature 550^{0}C and all films are phase pure. The ferroelectric property, dielectric property and leakage conduction property was studied. The film on LaNiO$_3$ bottom has most intense ferroelectricity and show a 2Pr of 6.61µC/cm^2. The 2Pr are 4.53 µC/cm^2 and 4.14µC/cm^2 for the film on Pt and ITO bottom electrodes. Accordingly, the film on LaNiO$_3$ bottom electrode has most intense dielectric property. The films on ITO and Pt bottom electrodes show small dielectric dispersion and it is attributed to good interface property. In the film on ITO bottom electrode, least current density was observed at the same applied field and it is attributed the compact intermediate layer.

ACKNOWLEDGMENTS

The work is supported by Middle-Aged and Young People Excellent Innovation Team of Science and Technology of Hubei Province under grant no. 2003–7 and the major project of Hubei normal university.

REFERENCES

[1] J.Wang, J.B.Neaton, H.Zheng; Science, **299**, 1791 **(2003)**.
[2] M.Fiebig, T.Lottermoser, D.Frohlich, A.V.Goltsev, R.V.Pisarev; Nature, **419**, 818 **(2002)**.
[3] M.M.Kumar, V.R.Palkar, K.Srinivas, S.V. Suryanarayana; Appl.Phys.Lett., **76**, 2764 **(2000)**.
[4] F.Zavaliche, P.Shafer, R.Ramesh; Appl.Phys.Lett., **87**, 252902 **(2005)**.
[5] I.Sosnowska, T.P.Neumaier, E.Steichele; J.Phys.C., **15**, 4835 **(1982)**.
[6] M.M.Kumar, A.Srinivas, S.V.Suryanarayana; J. Appl.Phys., **87**, 855 **(2000)**.
[7] J.R.Teague, R.Gerson, W.J.James; Solid State Commun., **8**, 1073 **(1970)**.
[8] F.Kubel, H.Schmid; Acta Crystallogr. **46**, 698 **(1990)**.
[9] J.Li, J.Wang, M.Wuttig, R.Ramesh, N.Wang, B.Ruette, A.P.Pyatakov, A.K.Zvezdin, D.Viehland; Appl.Phys.Lett., **84**, 5261 **(2004)**.
[10] K.Y.Yun, D.Ricinschi, T.Kanashima, M.Noda, M. Okuyama; Jpn.J.Appl.Phys., **L243**, 647 **(2004)**.
[11] S.K.Singh, H.Ishiwara; Jpn.J.Appl.Phys., **L244**, 734 **(2005)**.
[12] W.Eerenstein, F.D.Morrison, J.Dho, M.G.Blamire, J.F.Scott, N.D.Mathur; Science, **307**, 1203a **(2005)**.
[13] X.J.Meng, J.G.Cheng, J.L.Sun, H.J.Ye, S.L.Guo, J.H.Chu; J.Cryst.Growth, **220**, 100 **(2000)**.
[14] Z.Liu, H.Liu, G.Du, J.Zhang, K.Yao; J.Appl.Phys., **100**, 044110 **(2006)**.
[15] J.Wang, X.G.Tang, H.L.W.Chan, C.L.Choy, H.Luo; Appl.Phys.Lett., **86**, 152907 **(2005)**.
[16] S.Chopra, S.Sharma, T.C.Goel, R.G.Mendiratta; Solid State Commun., **127**, 229 **(2003)**.
[17] V.R.Palkar, J.John, R.Pinto; Appl.Phys.Lett., **80**, 1628 **(2002)**.
[18] K.Y.Yun, M.Noda, M.Okuyama; Appl.Phys.Lett., **83**, 3981 **(2003)**.